Effect of temporal and spatial asymmetries to the neuromuscular control of the lower limbs during stationary cycling

Magdalena Zych[1], Ian Rankin[2], Donal Holland[2], Giacomo Severini[1*]

[1]School of Electrical and Electronic Engineering, University College Dublin, Belfield, Dublin 4, Dublin

[2]School of Mechanical and Materials Engineering, University College Dublin, Belfield, Dublin 4, Dublin

Running Head***: Motor adaptations during asymmetric cycling***

Correspondence:

Giacomo Severini, PhD

School of Electrical and Electronics Engineering,

University College Dublin,

Belfield, Dublin 4,

Ireland

giacomo.severini@ucd.ie

Abstract

Motor adaptations are a useful tool in the study of the neurophysiology and motor control of the lower limbs. However, motor adaptation paradigms for the lower limbs are typically based on locomotion tasks, where the necessity of maintaining a stable gait pattern is the main driver of adaptations and could possibly mask other underlying processes. The aim of this study was to investigate whether small temporal or spatial asymmetries can trigger motor adaptations during stationary cycling tasks where stability is not directly compromised. Therefore 14 healthy individuals participated in two experiments: in one the angle between the crank arms of the pedals was altered by 10° to induce a temporal asymmetry; in the other the length of one pedal was shortened by 2.4 cm to induce a spatial asymmetry. We recorded the acceleration of the crank arms during the exercises and the EMGs of 16 muscles. The analysis of the accelerometer data was used to investigate the presence and extent of motor adaptations. Muscle synergies analysis was used to quantify changes in neuromuscular control. We found that motor adaptations are present in response to temporal asymmetries. This adaptation was obtained, at the neuromuscular level, mostly by rotating two synergies on the perturbed side. Spatial asymmetries, on the other hand, appear to trigger a feedback-driven response that does not present an aftereffect and is not consistent with a motor adaptation. All the changes in neuromuscular control were well explained by changes in recruitment of a fixed set of muscle synergies.

New and Noteworthy

The processes driving lower limb motor adaptations are not fully clear, as such adaptations are mainly driven by stability. Here we show that lower limb adaptations can be obtained also in the absence of an explicit balance threat. We also show that adaptations are present also when kinematic error cannot be compensated for, suggesting the presence of intrinsic error measures regulating the timing of activation of the two legs.

Keywords

Motor Adaptations; Muscle Synergies; Central Pattern Generators;

Introduction

When performing repetitive movements such as walking and cycling, the human central nervous system coordinates different neural commands to form patterns of alternating muscular activations that are mostly automated. The planning and voluntary adjustments of the motor plan take place in supraspinal areas and the cortex (Caggiano et al. 2018; Drew 1988; Jordan et al. 2008; Takakusaki 2013) while the muscular pattern formation and the timing of activation is mostly regulated at the spinal level (Grillner 2003; Kiehn 2016; 2006). During walking, if a sudden obstacle or a continuous perturbation disrupts the task in a relevant way, these automated patterns are modulated to overcome or reject the disturbance. Fast interferences (e.g. tripping into an obstacle or slipping on a slippery surface) are compensated through fast spinal reflex responses (McDonagh and Duncan 2002; Schillings et al. 2000; van der Linden et al. 2007), while continuous perturbations or modifications of the movement environment require for the motor plan to be progressively updated to reject the error in a phenomenon often referred to as locomotor adaptation (Torres-Oviedo et al. 2011).

While our knowledge of spinal reflexes and their role during locomotion is substantial (Kandel et al. 2000; Pearson 2004), the processes behind the generation of locomotor adaptations are not fully understood yet. Most of our knowledge on lower limb and locomotor adaptations derives from studies based on actual walking disturbances administered either using robotic systems (Cajigas et al. 2017; Emken et al. 2007; Emken and Reinkensmeyer 2005) or by altering the walking environment, such as in the split-belt treadmill paradigm (Choi and Bastian 2007; Prokop et al. 1995; Reisman et al. 2005). These studies have shown that motor adaptations during locomotion are generated mostly to maintain gait stability (Cajigas et al. 2017; Lam et al. 2006; Prokop et al. 1995), to reduce energy consumption (Emken et al. 2007; Finley et al. 2013) and due to a natural bias towards symmetry (Reisman et al. 2005). A recent work has shown that stability has primacy over the other drivers of adaptation (Cajigas et al. 2017), whereas perturbations altering stability are compensated even if they lead to an increased energy consumption while perturbations that do not alter stability are ignored in favour of a more economical gait pattern. Nevertheless, it is still not fully clear which circuits are adapted during locomotor adaptations and, since most experimental paradigms alter the balance requirements during

the task, if such adaptations are hardwired or a response to a behavioral trigger such as maintaining a long term stable gait pattern.

This latter point is specifically of interest given the fact that locomotor adaptations have proved to be a valuable tool for clarifying the organization of the neural circuits controlling the lower limbs during repetitive movements in humans. As an example, seminal work by Choi and Bastian (Choi and Bastian 2007) used the split-belt treadmill paradigm to study the organization of the hypothetical Central Pattern Generator (CPG) circuits in the human spinal cord. Such CPG circuits have been proposed as constituted by spatial components coordinating the activity of the different muscles together and rhythmic components coordinating the timing of activation of the spatial components (Kiehn 2006; McCrea and Rybak 2008; Zhong et al. 2012). Several studies have proposed that muscle synergies extracted by applying factorization algorithms to datasets constituted by large numbers of EMG signals may functionally model the two-layer structure of the CPGs in humans (Dominici et al. 2011; Ivanenko et al. 2005; Lacquaniti et al. 2012; Maclellan et al. 2014).

In this work we propose a novel method for the study lower limb motor adaptations based on asymmetric cycling. In this method we introduce small temporal or spatial asymmetries in the cycling pattern of healthy individuals during exercises on a stationary bike to verify the presence and study the neuromuscular correlates of locomotor adaptations (Maclellan et al. 2014). Temporal asymmetries are introduced by slightly altering the relative angle between the crank arms of the cycling system, while spatial asymmetries are introduced by altering the length of one of the two crank arms. This approach allows us to study automatic reactions, if any occur, to alterations in the normal temporal and spatial organization of repetitive lower limb movements without introducing perturbations that may directly affect balance. Conceivably, introducing an asymmetry in the timing of activation of the two legs disrupts the coordination of the rhythmic components of the CPGs. On the other hand, the spatial asymmetry modifies the muscular requirements for the task and may translate in modifications in the layer of the CPGs regulating the co-recruitment of the different muscles. Observing motor adaptations in one or both of these components may help to identify which of the neural circuits that control lower limb movements are automatically adapted even in the absence of a behavioral primer such as a balance

threat. Herein we studied the presence of motor adaptation during the previously described two asymmetric cycling tasks by tracking changes in acceleration patterns in the crank arm and in the temporal and spatial components of the muscle synergies (d'Avella et al. 2003) associated with both experiments. This latter analysis is used as an insight in the activity of the different components of the CPGs controlling the lower limbs.

Materials and Methods

Participants. Fourteen healthy individuals (7 females; 26.1 ± 3.0 years old, 171.6 ± 6.7 cm, 64.2 ± 7.3 kg) volunteered to participate in the experiments. All participants reported their right leg to be the dominant one, intended as the leg they would use to kick a ball. Inclusion criteria consisted of the absence of neurological, orthopaedic or cognitive impairment that would in any way affect the execution of the experiment. Only two out of fourteen subjects routinely used clipless pedals when cycling (recreationally or for commute), while all the others utilized standard pedals.

All the experimental procedures described in the following have been approved by the Ethical Committee of University College Dublin and has been conducted according to the WMA's declaration of Helsinki. All subjects gave written informed consent before participating in this study.

Experimental Procedures. All tests were performed by each participant in a single experimental session. Participants were instructed to refrain from vigorous physical activity within 2 hours before testing. During the experimental session each participant underwent two sessions of cycling, each relative to a different symmetry perturbation. All cycling exercises were performed using a standard training cycloergometer (Lode BV, Groningen, The Netherlands). The pedals of the cycloergometer were equipped with straps that were used to solidly attach the feet of the subjects to the pedal during the experiments.

One symmetry perturbation (Angle experiment) consisted in a 10° clockwise modification in the angle between the two crank arms. This was achieved by mean of a custom metal attachment directly connected to the end of the right crank arm (**Figure 1**). The other symmetry perturbation (Length

experiment) consisted in a shortening of the right crank arm by 2.3 cm. This was obtained by attaching a commercial shortening system (Pulse Crank Shortener Highpath Engineering Ltd., Tring, UK) to the right crank arm (**Figure 1**). In both experiments participants were asked to cycle for 5 minutes without asymmetries (baseline, BL), followed by 10 minutes of asymmetric cycling (adaptation, AD) and concluded each experiment with 5 minutes of symmetric cycling (post-adaptation, PA, **Figure 1**). Between each phase of each experiment the participants were allowed 5 minutes of rest, that were used to modify the pedal setup (e.g. to add or remove the asymmetries). Participants were specifically asked not to walk during the resting period between AD and PA to avoid possible washouts. Between the two experiments each participant was given a 20 minutes break. The order of the two experiments was randomized across subjects with half subjects performing the Angle experiment first. In all sessions of both experiments the cycloergometer was set at a constant torque equal to 6.5 Nm. This value was chosen so to keep the participant engaged while minimizing the possibility of muscle fatigue. Subjects were asked to reach as soon as possible and maintain a recreational pace of 75 revolutions per minute (rpm) during all phases of the experiments. Visual feedback on their pace was presented to them on the digital screen of the cycloergometer. Before the beginning of the first experiment the position of the saddle was adjusted to 109% of the inseam length between saddle and pedal in a pushed down position. This distance ensures optimal performance and safety for the locomotor system (Hamley and Thomas 1967; Peveler et al. 2007).

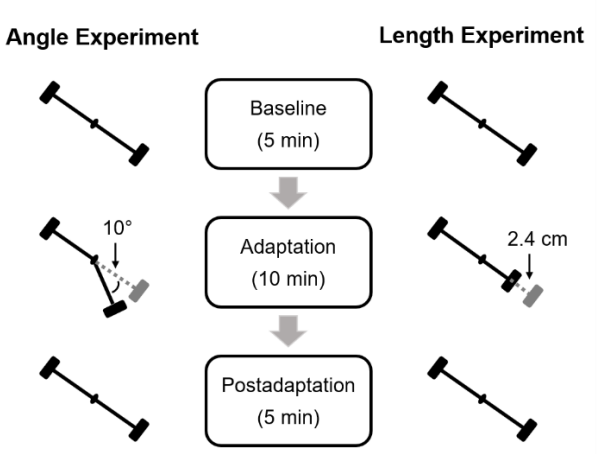

Fig 1. Experimental setup. The figure shows a representation of the lateral view of the crank arms and pedals during the different phases of the two experiments. The asymmetry in the Angle experiment consisted of a 10 degrees clockwise deviation in the relative angle between the crank arms of the cycloergometer. The asymmetry in the Length experiment consisted in a 2.4 cm shortening of the right crank arm. Both experiments consisted of 5 minutes symmetric cycling (baseline), followed by 10 minutes of asymmetric cycling (adaptation) and 5 minutes of symmetric cycling (postadaptation).

Data recoding. The activity of 16 muscles was recorded during both experiments using surface electromyography (sEMG). The electrode placement was performed at the beginning of the experimental session and data quality was checked through the different phases of both experiments. Wireless EMG sensors (Trigno Flex, Delsys, Boston, MA) were placed bilaterally (after the skin was prepared using alcohol), according to the SENIAM recommendations (Hermens et al. 1999), on the rectus femoris (RF), vastus lateralis (VL), tensor fasciae latae (TFL), gluteus maximus (GMax), biceps femoris (BF), tibialis anterior (TA), soleus (Sol) and gastrocnemius medialis (GM). The sampling frequency for the EMG sensors was set to 2000 Hz. One accelerometer (Trigno Flex sensors, Delsys, Boston, MA) was also placed on the right crank arm and sampled at 148 Hz. A custom 6 cm flexible bend sensor was mounted under the left pedal in a bottom down position, so that the top 2 cm would bend each time the pedal was in its lowermost position. The data from the bend sensor were also sampled at 148 Hz and were used to determine the beginning of each cycle. All the sensors (EMG, accelerometers and bend sensors) where acquired synchronously using a custom Labview (Labview 2012, National Instruments, Austin, TX) software.

Analysis of accelerometer data. All analysis routines were performed offline in MATLAB (MathWorks, Natick, MA). Biomechanical changes due to the introduction of the pedal asymmetries were estimated from the data from the accelerometer unit attached to the right crank arm. The *x* and *y* components (where *x* indicates the anteroposterior and *y* indicates the vertical direction) of the accelerometer data were segmented into individual cycles, identified as the interval between consecutive spikes in the flex sensor indicating the left pedal reaching the dead bottom of its trajectory, and length normalized to 100

points. The tangential vector of the acceleration was then computed for each segment as the square root of the sum of the squares of the *x* and *y* components of acceleration. As both the speed and the torque of each cycling exercise was fixed, changes in the accelerometer data were investigated as changes in the shape of the tangential acceleration pattern across the different cycles. Specifically, we used as metric the position of the minimum tangential acceleration that was determined to be robust in capturing asymmetry-driven changes in preliminary analyses (data on other metrics not shown). To investigate for possible exponential adaptive behaviors, as the one usually expected during locomotor adaptation and washout of adaptation (Cajigas et al. 2017), an exponential function was fitted on the median (across subjects) data from the adaptation and post-adaptation phases. The exponential function was fitted using a least square method and was in the form:

$$f(x) = \alpha \cdot e^{-\beta x} + \gamma \quad (1)$$

The time constant of the exponential, intended as the number of cycles needed for the exponential to reach its plateau, was estimated as $3/\beta$. We also analysed for differences in the position of the peak acceleration during different phases of the experiments, nominally late baseline, early adaptation, late adaptation and early post-adaptation. In this and all subsequent analyses "early" sections were constituted by the average of the first 50 cycles while "late" sections by the average of the last 50 cycles of a specific phase of each experiment.

EMG data processing and muscle synergies estimation. The recorded EMG signals were bandpass filtered (30-450 Hz) with a 4th-order band-pass Butterworth filter and rectified. The EMG envelopes were obtained from the data by filtering with a 3rd-order low-pass Butterworth filter with cut-off frequency of 5 Hz. The envelopes were then segmented into individual cycles using the same procedure utilized for segmenting the accelerometer data. Cycles with artefacts or abnormal spiking activity were removed from subsequent analyses. All cycles of each channel were then amplitude normalized by dividing them by the average maximal value of the envelopes calculated from all the cycles from the baseline phase of each experiment. All the segmented cycles were then length-normalized by interpolating them to 100 points over a cycle. Muscle synergies were then extracted using the Non-

Negative Matrix Factorisation (NNMF) algorithm (Lee and Seung 2001). The algorithm decomposes the matrix of EMG envelopes as:

$$E = W \cdot H + r \quad (2)$$

where E is a $m \times t$ envelope matrix (m – number of muscles, t – number of samples used); W is a $m \times s$ synergy vectors matrix (s – number of modules) containing the relative weights of each muscle within each synergy; H is a $s \times t$ activation pattern (AP) matrix; r is a root mean square residual error that describes difference between reconstructed envelope matrix and original one. The NNMF algorithm was applied to epochs consisting of consecutive bouts of 10 cycles concatenated together. The quality of reconstruction was measured using the variance accounted for (VAF):

$$VAF = 1 - \frac{SSE}{SST} \quad (3)$$

where SSE is sum of squared errors and SST is total sum of squares (Torres-Oviedo et al. 2006). Previous studies in literature have found that cycling is well described by using either 4 or 5 modules (Barroso et al. 2014; De Marchis et al. 2013; De Marchis et al. 2015). We performed synergies analysis by extracting 4 and 5 modules and selected the most appropriate reconstruction for further analysis as the one yielding an average VAF across subjects >90% and >80% for each muscle.

Analysis of the changes in muscle synergy shape and activation patterns. To assess for differences in the shape of the synergy weights through the different phases of both experiments we compared the contribution of each muscle to each synergy during late baseline, early adaptation and late adaptation. To capture overall changes in the composition of the synergy modules we also calculated the normalized dot product between the average set of weights estimated during all the epochs of baseline and those estimated in late baseline, early adaptation and late adaptation. As changes in the accelerometer were characterized by a shift in the peak of the acceleration of the crank arm, we assessed for shifts of the APs during the course of the two experiments. This analysis was based on the calculation of the lag of the cross-correlation function between the average AP of each synergy calculated during BL and the APs extracted from each epoch. We also compared, for each synergy, the average lag calculated at late baseline, early adaptation, late adaptation and early post-adaptation. As a final analysis, we assessed for

changes in the intensity of synergies APs through the experiments. This analysis was based, for each epoch of each leg, on the calculation of the average (across synergies) absolute variation in the RMS of the APs with respect to whole baseline (excluding the first epoch). Linear or exponential functions (in the form expressed in equation 1) were fitted on the data relative to BL, AD and PA of each experiment separately using a least squares approach. We also compared the values of RMS between the first epoch of BL, AD and PA for both legs in both experiments.

Statistical Analyses. A series of statistical analyses was performed to assess for differences in the parameters calculated from the different signal across the different phases of each experiment. Changes in the average position of the peak acceleration were evaluated, across the different phases of both experiment s, using Friedman's test and a post-hoc analysis based on Dunn-Sidak's criterion (non-normality of the data was assessed using the Kolmogorov-Smirnov test). Similarly, the same statistical analysis was used to assess for changes in the individual muscle weights through the different phases of each experiment, the normalized dot product across the muscle weights, the lags of the APs for each synergy and the values of cumulative RMS in the first epoch of BL, AD and PA for both legs and experiments. For these cases also, the non-normality of the data was evaluated before the analysis. For all tests the significance level was set to $\alpha = 0.05$. Bonferroni's correction was applied to account for multiple comparisons.

Results

All accelerometer and EMG data were checked for quality before analysis. Subjects with poor EMG or accelerometer data were excluded from the final analyses. After this assessment, three subjects were dropped in the analysis of the accelerometers for both experiments, while one subject was excluded from the synergies analysis of the Angle experiment and two subjects were excluded from the analysis of the Length experiment. None of the subjects reported exhaustion or fatigue at the end of each phase of the experiments.

*Accelerometers***.** The results of the analysis of the accelerometer data are presented in **Fig. 2**. In both experiments we observed shifting patterns in the profile of the tangential acceleration of the right crank arm during the different phases of the experiments (**Figures 2A** and **2D**). Changes in magnitude in the acceleration were observed in the first two to five cycles of all three phases (as the subjects reached the required pace/power output) of the experiment and were consistent across all phases and experiments. This behavior is observable in **Figures 2A** and **2D** for the early adaptation data.

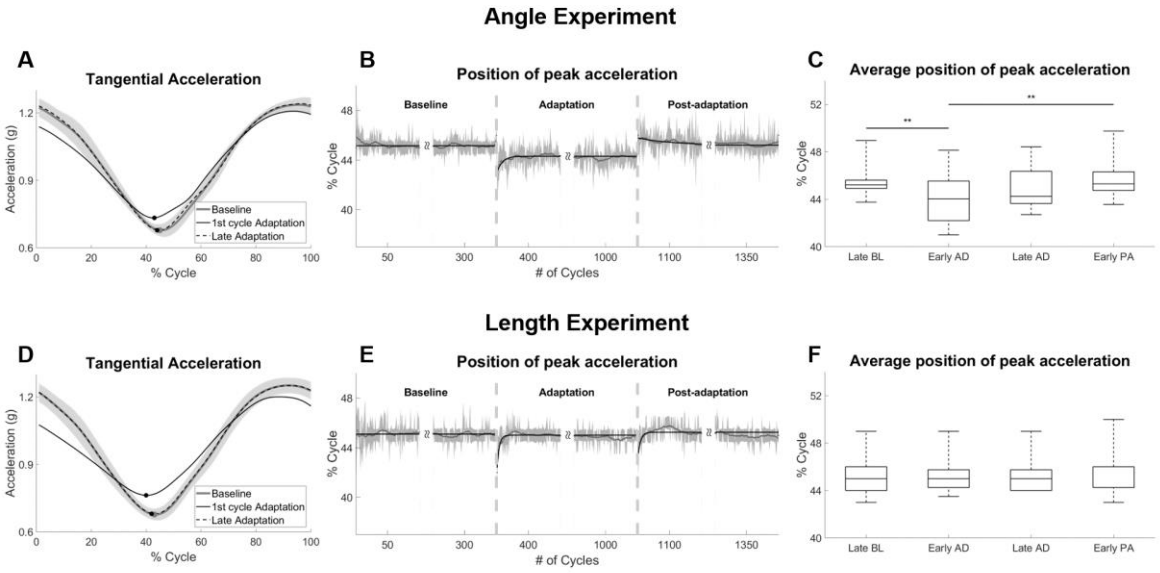

Fig 2. Changes in the profile of the tangential acceleration. Adaptation in the acceleration was characterized by tracking the changes in the position of the peak tangential acceleration. In *A* and *D* the shaded area represents the average ± standard deviation (across subjects) of the average tangential acceleration recorded during BL. Solid line represents the tangential acceleration in the first cycle of adaptation while the dashed line represents the average tangential acceleration at late adaptation (last 50 cycles). Bold markers represent the position of the minima for the three curves. In *B* and *E* the shaded area represents the median ± standard error values of the position of peak tangential acceleration through all the cycles of the experiments. The bold lines represent linear/exponential fitting (in the form presented in equation 1) of the median data. In *C* and *D* each boxplot represents the median, 25th and 75th percentiles, minimum and maximal values of the position of the peak tangential acceleration across the subjects on the data averaged across different phases of the two experiments. Late BL and Late AD refer to the last 50 cycles of BL and AD while Early AD and Early PA refer to the first 50 cycles of AD and PA. ** indicates statistical significance with p<0.01 according to Dunn-Sidak's method.

In the Angle experiment we observed a shifting pattern in the profile of the accelerometer data. This behavior was well captured by tracking the position of the minimum of the tangential acceleration pattern for each cycle and is consistent with an exponential adaptation and washout. The position of the peak acceleration was observed to be stable around a constant value (45.2 ± 1.6 % of the cycle) during the BL phase of the experiment (**Figure 2B**) and to shift earlier in the cycle at the beginning of the AD phase (41.7 ± 2.8 % in the first cycle of AD). The peak of acceleration progressively shifted back in the cycle until it reached a plateau at about 44.5 % of the cycle towards the end of the AD phase. This behavior can be modelled by an exponential function in the form presented in equation (1) and with a time constant (intended as the number of cycles that are necessary to reach the plateau from the beginning of adaptation) equal to 25 cycles (see **Table 1**). At the beginning of the PA phase we observed an after-effect opposite in direction with respect to the original peak shift observed at the beginning of AD. This translates in a shift forward in the peak of the acceleration up to about 46.0% of the cycle. We observed a slow exponential behavior (time constant equal to 166 cycles) related to the washout of the adapted behavior. Statistical analysis showed (**Figure 2C**) the position of the acceleration peak to be significantly lower ($p = 0.01$ in the post-hoc analysis) during early adaptation with respect to both late baseline and early post-adaptation.

Table 1. Exponential fitting parameters for position of the peak tangential acceleration for the AD and PA phases of the Angle and Length experiments. All values are presented together with ± 95% confidence intervals.

		α	β	γ	Time Constant
ANGLE	**AD**	-1.43 (-1.58, -1.27)	0.120 (0.102, 0.138)	44.31 (44.3, 44.32)	25.00 (21.74, 29.41)
	PA	0.59 (0.55, 0.64)	0.018 (0.015, 0.021)	45.20 (45.17 45.22)	166.67 (142.86, 200.00)
LENGTH	**AD**	-3.49 (-3.71, -3.27)	0.285 (0.263, 0.307)	45.01 (45.01, 45.02)	10.52 (9.77, 11.41)
	PA	-2.51 (-2.91, -2.11)	0.259 (0.206, 0.312)	45.25 (45.22, 45.27)	11.58 (9.62, 14.56)

In the Length experiment we again observed an exponential shift in the peak of the tangential acceleration (**Figure 2E**) during the adaptation phase. As for the Angle experiment, BL was characterized by consistent values of peak acceleration (45.2 ± 1.6 % of the cycle). At the beginning of the AD phase we observed an initial anticipation in the peak value of acceleration (42.4 ± 7.0 % in the first cycle of AD) that was exponentially shifted back close to the BL value by the end of AD. The time constant for this exponential behavior was estimated to be equal to 10 cycles (**Table 1**). At the beginning of PA, instead of an after-effect opposite to the original error at the beginning of AD as expected in a motor adaptation model and as observed in the Angle experiment, we observed once again a backward shift in the peak of the acceleration, in a behavior almost identical to the one observed during the AD phase. This exponential behavior was characterized by a time constant of about 11 cycles, similar to the one observed in the AD phase. Statistical analysis on the first/last 50 cycles of the different phases did not show statistically significant differences in the average position of the peak acceleration, as the initial changes in peak position at the beginning of AD and PA were not captured in this analysis due to the shortness of the relative exponential behaviors (10 cycles, against a window of analysis of 50 cycles) and to the fact that the initial shift was perfectly compensated for.

Muscle Synergies Analysis. In our analysis we compared the quality of EMG reconstruction after extracting either 4 or 5 synergies (**Figure 3A**), that are model orders commonly used in synergy analysis during cycling (Barroso et al. 2014; De Marchis et al. 2013). We found that 4 synergies yielded VAF values of 84.0% for the Angle experiment and 84.9% for the Length experiment, while 5 synergies values of VAF equal to 91.3% and 91.9% respectively for the two experiments. Based on these results we decided to perform all further analysis on the 5 synergies reconstruction. The synergy sets we extracted (**Figure 3B**) are in line with those found in similar works in literature (Barroso et al. 2014; De Marchis et al. 2013; De Marchis et al. 2015) and are constituted by the following modules: Synergy 1 is constituted by the quadriceps muscles (RF and VL) and hip extension in the first quadrant of the cycle (taking as starting point the highest position of the pedal during the cycle); Synergy 2 is constituted by

the muscles of the calf (Sol and GM) and controls ankle dorsiflexion in the second quadrant of the cycle; Synergy 3 is mostly constituted by the activity of the BF and GM and is also active in the second quadrant, controlling ankle dorsiflexion and knee extension; Synergy 4 is constituted by the TFL and the GMax and controls hip extension in the third quadrant; Synergy 5 is constituted by the TA and is mostly active in the fourth quadrant and is relative to ankle plantarflexion.

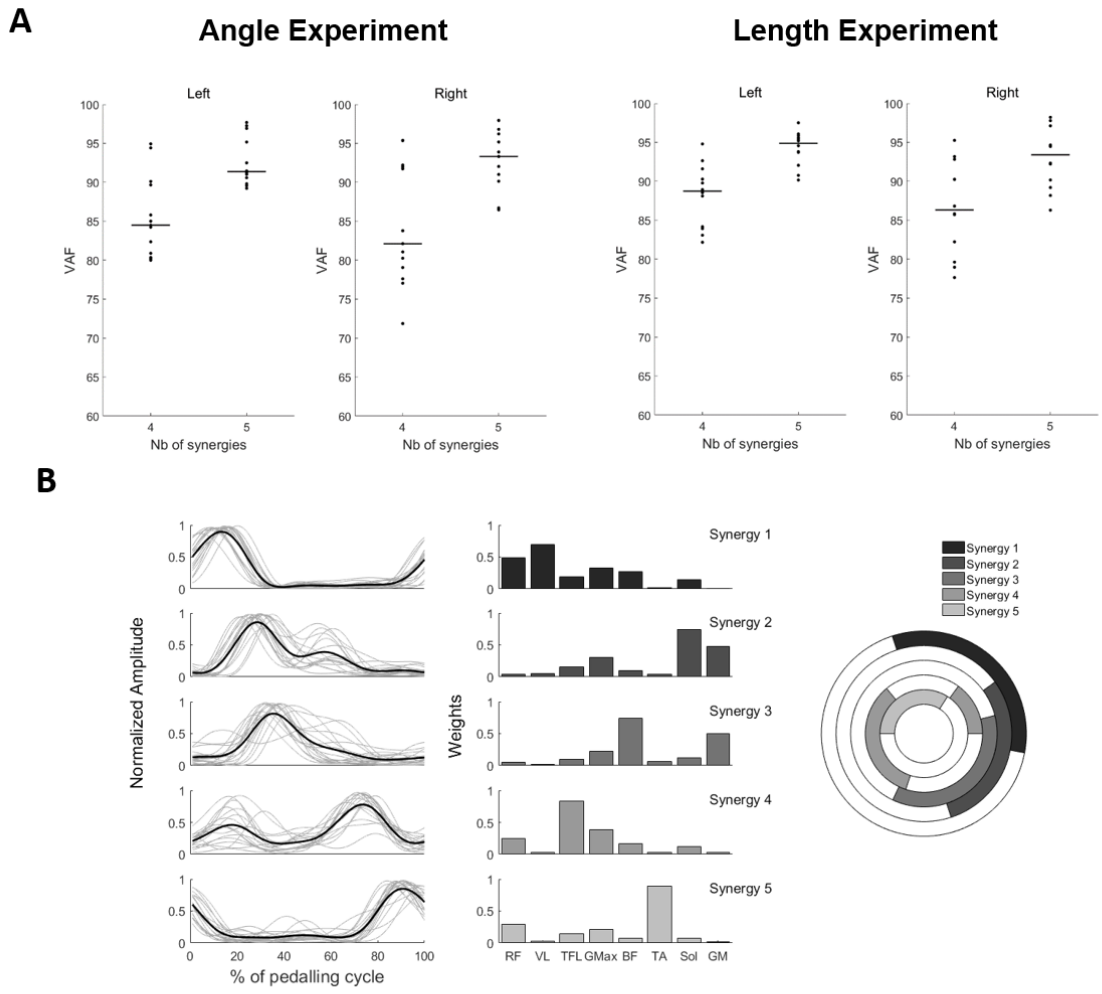

Fig 3. Muscle Synergies Extraction. In *A* are shown the values of VAF obtained by extracting either 4 or 5 synergies from the data recorded at baseline from both legs of the participants. Individual dots represent individual subjects, while horizontal lines represent average values across subjects. In *B* are shown, from left to right, the activation patterns of the 5 synergies (bold lines represent the average across subjects, light

lines represent individual subjects), the average weights recorded across subjects and the activation patterns as mapped in a circle representing the position of the foot during a cycle.

Changes in Synergy Modules and Activation Patterns. We analysed the changes in synergies modules and APs through the different phases of the two experiments to capture specific neuromuscular behaviors consistent with the biomechanical changes we observed in the analysis of the accelerometers.

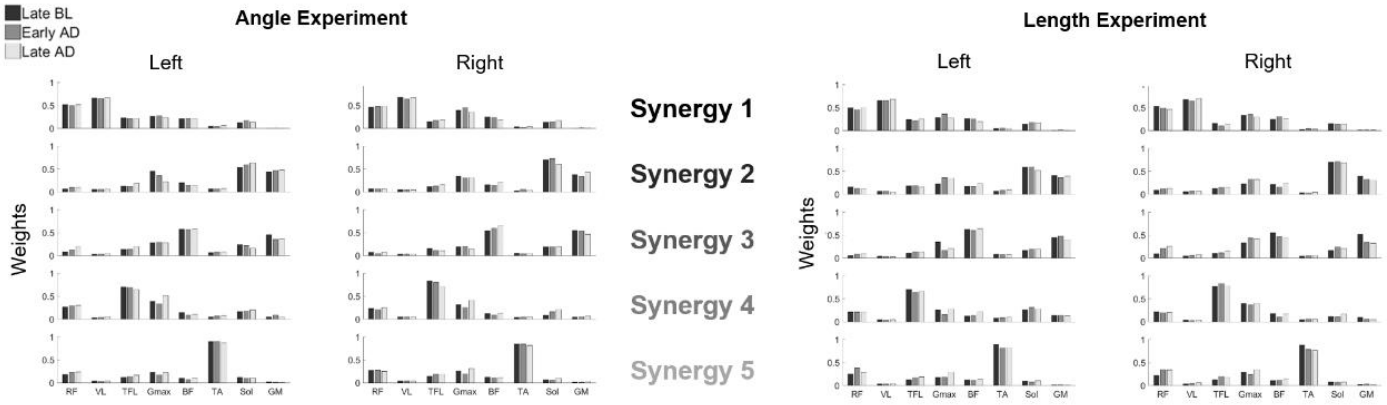

Relative to the composition of the motor modules, we did not observe statistically significant changes in the representation of each muscle in each module during late baseline, early adaptation and late adaptation (**Figure 4**). Although the weights of each muscle in each synergy were shown to fluctuate slightly through the different phases, none of the changes were statistically significant.

Fig 4. Synergy modules across the different phases of each experiment. Each bar represents the average (across subjects) value of the contribution of a muscle to each synergy (color coded as in Fig. 3) estimated across the different phases of the two experiments. Black represents Late BL, grey Early AD and light grey Late AD. No statistical differences were observed.

As a cumulative analysis of the changes in the shape of the synergy modules, we calculated the average normalized dot product between the modules estimated through all baseline and those estimated in late

baseline, early adaptation and late adaptation (**Figure 5**). This metric has been often used to capture overall changes in the shape of muscle synergies (Tresch et al. 1999). Also in this case we did not observe statistically significant changes, indicating an overall consistency of the motor modules between BL and AD.

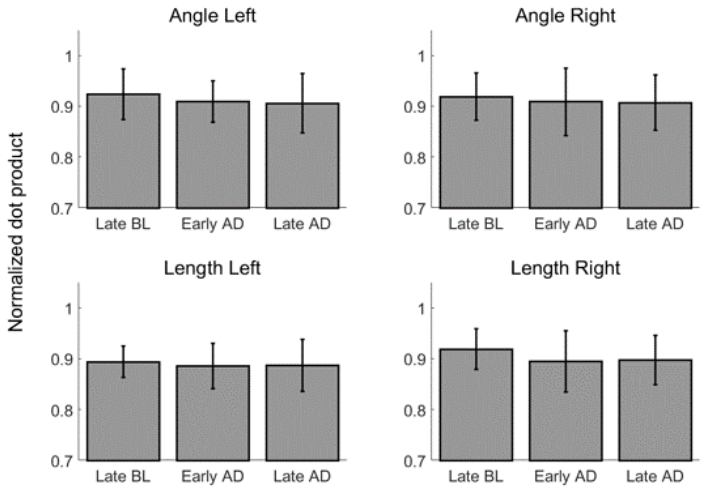

Fig 5. Differences in module similarity. Each bar represents the average (across subjects) ± standard deviation value of normalized dot product between the average synergy weights estimated from all epochs of BL and those estimated in Late BL, Early AD and Late AD. We did not observe statistically significant differences in any side or experiment.

In both experiments we observed qualitative changes in the APs of the synergies modules that were mostly characterized by small changes in amplitude and peak timing in the cycling pattern (**Figure 6A** and **6B**). In the Angle experiment, in a visual analysis of **Fig. 6A,** we noted progressive changes in APs amplitude in synergies 2, 3 and 4 on the left side and in all synergies on the right side. Moreover, we observed progressive shifts in the activation timing of the APs of Synergies 2 and 3 for the right side. These changes reflect a progressive anticipation of the activity of the calf muscles and of the BF during the cycle that possibly translates into an anticipation of ankle plantar flexion and knee flexion during the cycle, necessary to compensate the anticipation in peak acceleration. In the Length experiment we again observed progressive changes in synergy amplitude on most of the synergies on both sides, but

we did not observe clear shifts in the position of the APs. In order to capture quantitatively the shifting of the APs we calculated the lag of the cross-correlation functions between the average APs during BL and those calculated in all the epochs of the experiment (with particular focus on late baseline, early and late adaptation and early post-adaptation). In the Angle experiment (**Figure 7**) we did not observe shifts in the position of the APs for the synergies of the left leg, with median values of lags around 0 through all phases of the experiment for all the 5 synergies. On the right leg, however, we observed clear progressive shifts in AP position for synergies 2 and 3, as already qualitatively observed from **Fig. 6A**. For these synergies we observed a gradual anticipation of the APs during the AD phase that quickly stabilizes around a plateau value and is quickly washed out at the beginning of the PA phase. We observed statistically significant differences in lag between late adaptation and early post-adaptation in Synergy 2 and between late baseline and both early and late adaptation in Synergy 3. In the Length experiment (**Figure 8**) we did not observe shifts in the AP of all the synergies on both legs.

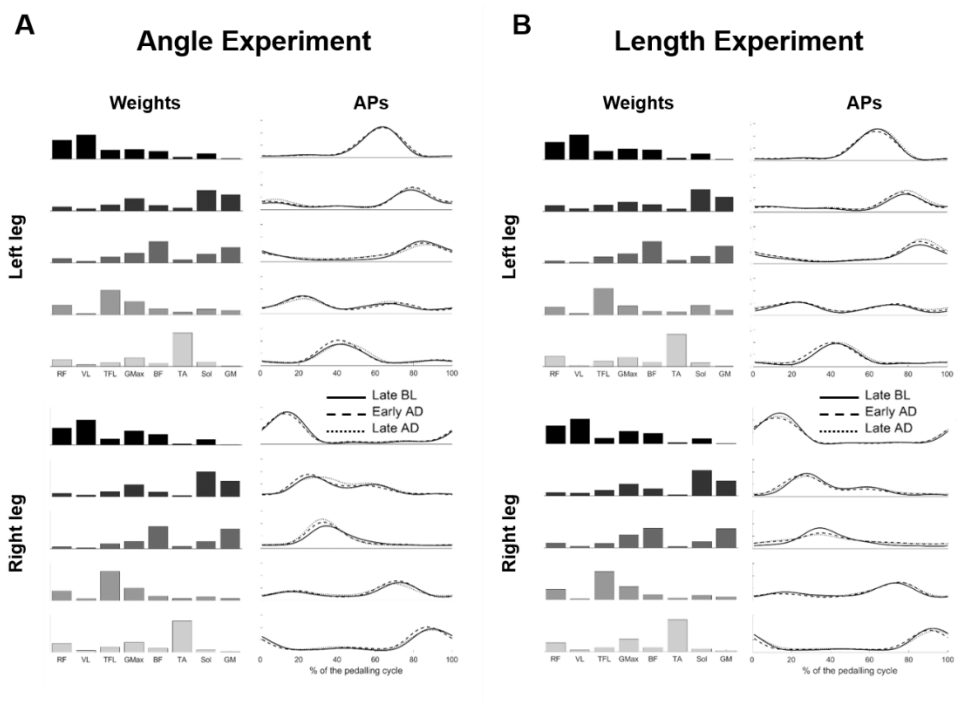

Fig. 6. Weights and APs of the muscle synergies across the different phases of the experiments. Panel *A* presents the results of the Angle experiment, panel *B* of the Length experiment. For each panel, top plots represent the left leg, while bottom plots represent the right leg. Synergies modules

are the average modules at baseline and are showed for reference. For each AP plot, the bold line represents Late BL, the dashed line represents Early AD and the dotted line represents Late AD.

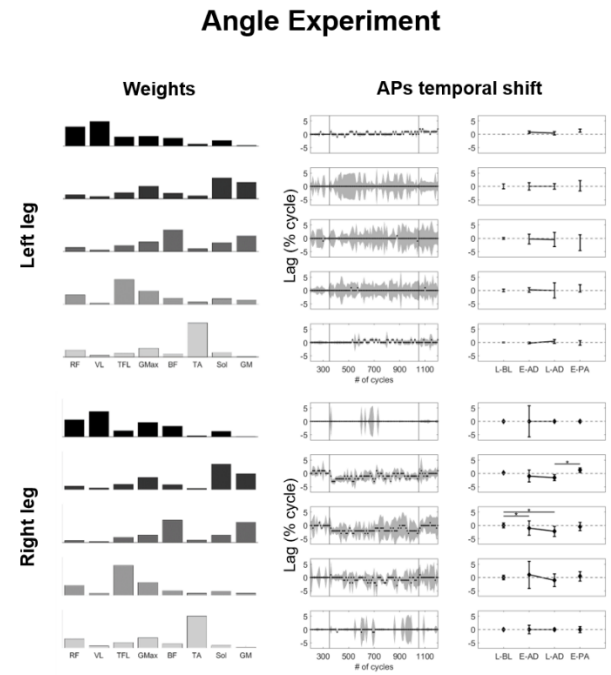

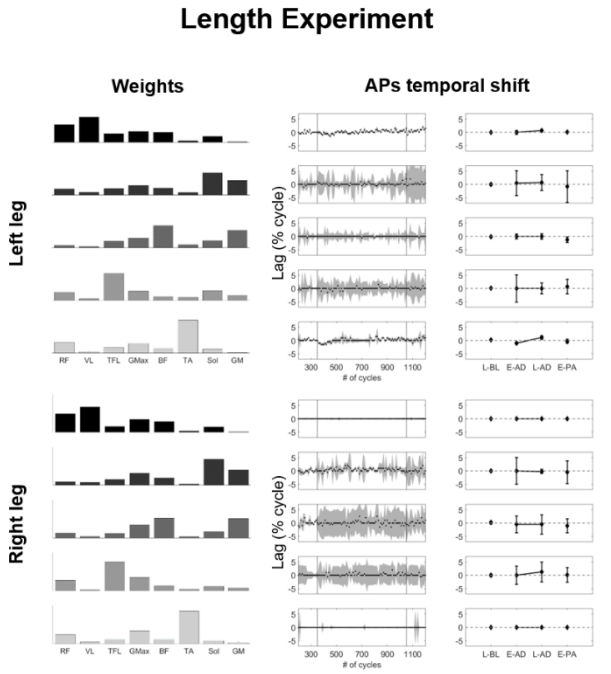

Fig. 7 and 8. Temporal shifts in the APs of the muscle synergies. Top plots present the results for the left leg, bottom plots for the right leg. The first row on the left presents the shapes of the muscle synergies during baseline (for reference). The middle row presents the lag between the average baseline APs and the APs of each epoch (expressed as median ± standard error across subjects), through all the experiment. Each point represents the median lag across subjects in one epoch, while the shaded area represents the standard error. The two vertical lines represent the beginning and end of the AD phase. The row on the right represents the average and standard deviation of the lag calculated during Late BL, Early AD, Late AD and Early PA. * indicates statistically significant differences with p<0.05 (based on Dunn-Sidak's method)

Finally, we analysed the changes in the RMS of the APs of the synergies extracted from both legs during the two experiments. In the Angle experiment (**Figure 9A**), for both legs, the data at baseline followed a negative linear trend, indicating a slight decrease in the overall activation of the synergies through the initial phase of the experiment that possibly reflects an ongoing habituation to the task. During the AD phase we observed an increase in the average RMS of the APs that follows an exponential pattern for both the left and the right leg (time constants equal to 55.1 and 27.5 epochs respectively). For both legs, post-adaptation was characterized by a slightly decreasing linear trend. We also observed that the first epoch of all three phases of the experiment are characterized by a higher intensity across the 5 synergies. This increase likely reflects the initial effort necessary to reach the required speed and was not shown to be statistically different between the three phases of the experiment (**Figure 9A**).

In the Length experiment (**Figure 9B**) we again observed a linear decrease in RMS in both legs during baseline, followed by an increase in RMS (linear for both legs) during adaptation and a slight decrease during post-adaptation. During the length experiment we observed an increase in RMS only in the first epoch of BL, while for the first epochs of both AD and PA we observed values in line with those observed in the adjacent epochs. The first epoch of the three phases of the experiment were shown to be statistically different across them with post-hoc analysis confirming differences between BL and both AD and PA. The lack of RMS increase at the beginning of AD and PA likely reflects the exponential

behaviors observed in the acceleration (**Figure 2**). In fact, the time constants of the exponentials are approximatively 10 cycles, that is the duration of one epoch in the synergies analysis.

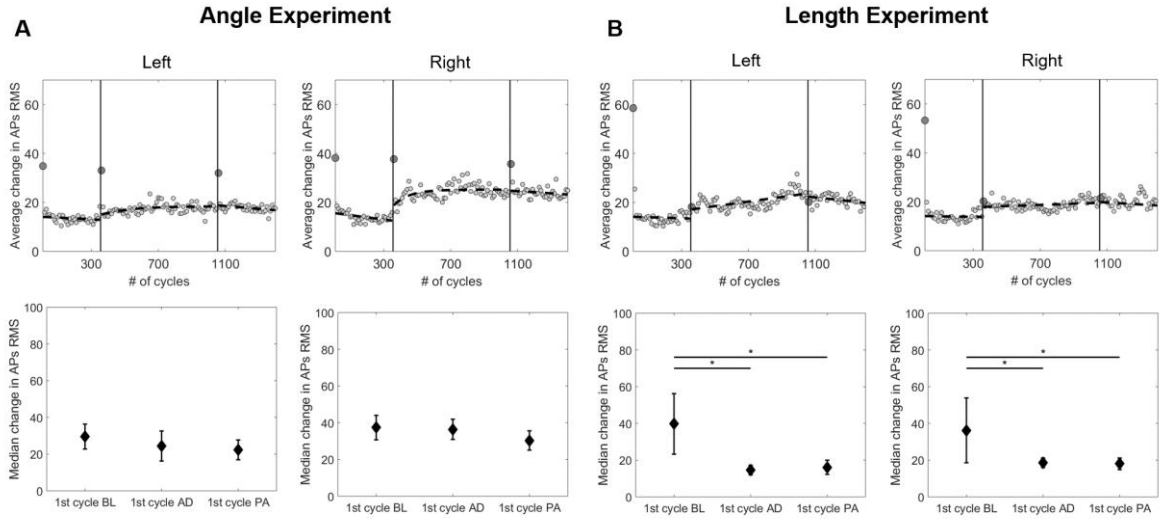

Figure 9. Cumulative changes in synergies RMS. Panel *A* presents the results of the Angle experiment, panel *B* of the Length experiment. For each panel, the plots on the left present the results for the left leg, the plots on the right for the right leg. Top plots present the average (across synergies) change in RMS for each epoch averaged across subjects. Individual points represent percentage changes for each epoch with respect to Late BL. The first epoch of each phase (BL, AD and PA) are presented with a darker point. Vertical lines represent the beginning and end of the AD phase. Bold dashed lines represent linear/exponential fits better representing the data. Bottom plots presents the median ± standard error across subjects of the change in RMS in the 1st epoch of BL, AD and PA. * indicates statistically significant differences with p<0.05 (based on Dunn-Sidak's method)

To better clarify this latter behavior, we analysed the shapes of the APs for all synergies extracted during the first epochs of BL, AD and PA in the Length experiment (**Figure 10**). As expected, during BL we observed an increase in RMS (characterized either by higher AP peaks or longer AP activation profiles)

in all synergies. On the other hand, we observed consistent behaviors between the two initial epochs of AD and PA, characterized by the absence of an increase or extension of the AP profiles that remained, for all synergies in both conditions, remarkably close to the normative represented by the average APs recorded during BL.

Discussion

In the two experiments herein presented, we investigated if small asymmetries in the angle and length of the crank arms of the pedals during cycling translate into motor adaptations. We found that altering the angle between the two pedals leads to a progressive shift in the crank acceleration that is consistent with a motor adaptation, intended as a progressive update of the motor plan, and presents an opposite after-effect once the asymmetry is removed. This adaptation appears to be mainly obtained by modulating the timing of activation of some of the synergies on the "perturbed" side. For the length asymmetry, we observed a behavior characterized by a fast exponential response that is equivalently (in magnitude, timing and side) observed in both adaptation and post-adaptation. This behavior appears to be caused by a re-modulation of the magnitude of the APs of the bilateral synergies in the first ten cycles of adaptation and post-adaptation. The lack of an opposite after-effect during post-adaptation suggests that this behavior is not consistent with a predictive motor adaptation.

*Angle experiment, insights into possible adaptation mechanisms***.** In the Angle experiment we observed an adaptation-like behavior that is reflected, at the biomechanical level, by a shift in the peak of the tangential acceleration of the crank arm. This adaptation converges in about 25 cycles, and is characterized, at the neuromuscular level, by a similarly timed exponential shift in the activation of the 2 synergies on the perturbed side, whose activation patterns peak at the dead bottom of the cycle, and by a slower bilateral exponential modulation of the synergies magnitude.

It is worth noticing that the exponential expression of motor adaptations is caused by the progressive decrease in biomechanical error driven by the cycle-by-cycle update of the internal models driving the task (Kawato 1999; Scheidt et al. 2001; Shadmehr and Mussa-Ivaldi 1994). In the Angle experiment the asymmetry introduces a fixed static alteration in the half-cycle relationship between the two legs

(Ivanenko et al. 2004), but since the kinematics of the movement cannot be altered, the kinematic error cannot be compensated over the course of the exposure to the experiment. Thus, our results point towards the presence of implicit kinetic or temporal error measures that are minimized during the AD phase. These error measures are likely driven by force and position proprioceptors (Jensen et al. 1998), that map the relative timing between the hypothetical CPGs driving the two legs similarly to what has been observed in cats (Frigon et al. 2013). This result is not unexpected as adaptation specific to temporal parameters of repetitive leg movements was also observed during split-belt treadmill experiments in humans (Malone et al. 2012).

The adaptation that we observed in the neuromuscular activity of the subjects during the Angle experiment is bilateral for what concerns the modulation of the synergies amplitude, while it is circumscribed to the "perturbed" leg in its temporal component. We did not observe bilaterally-linked temporal adjustments in the muscle synergies as previously observed in the split-belt treadmill experiment (Maclellan et al. 2014) although the synergies amplitude changes do not exclude possible bilateral mechanisms. Our results seem more in line with side-specific adjustments in the timing of the CPGs (Choi and Bastian 2007) that is, however, driven by a bias toward a fixed synchronization between the two legs (Reisman et al. 2005). As an additional remark on the Angle experiment, the adaptation behavior that we observe does not appear to follow an energy minimization principle (Finley et al. 2013), as we observe an overall increase in muscular activity during the AD phase (**Figure 9A**) of the experiment. Nevertheless, EMG analysis, although shown to be predictive of energy consumption in some scenarios (Abe et al. 2007) cannot be considered a direct measure of the metabolic cost of a task thus our results cannot fully substantiate this latter observation.

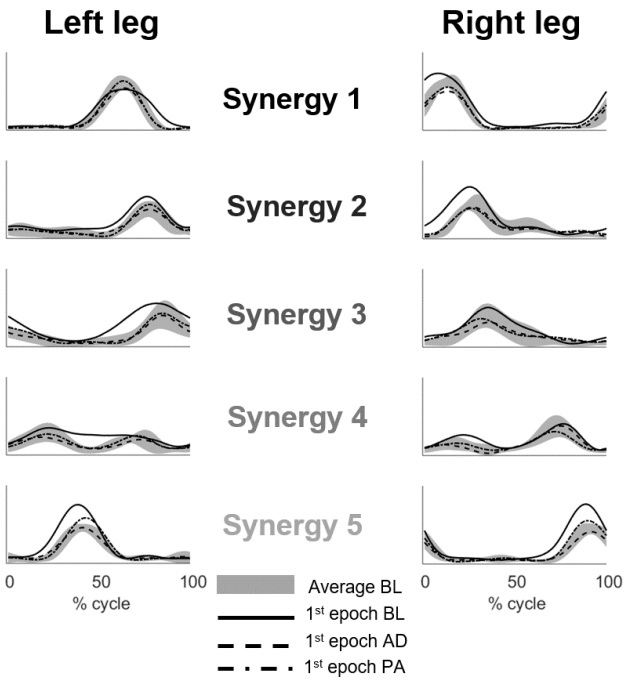

Figure 10. Synergies APs in the first epoch of BL, AD and PA for the Length experiment. For each plot, the shaded grey area represents the average AP calculated in BL (excluding the first epoch), the solid, dashed and dash-dotted lines represent, respectively, the first epoch of BL, AD and PA.

Length experiment, potential influence of spinal reflexes. In the Length experiment we observed, at the biomechanical level, an initial anticipation in the peak of the tangential acceleration of the crank arm that is quickly (time constant equal to 10 cycles) shifted back to its baseline value and does not present an opposite after-effect but an almost identical behavior also during PA. At the neuromuscular level, as expected, we did not observe noticeable temporal adjustments in the synergies APs (**Figure 7**), as the timing between the two legs had been left unaltered. We instead observed a systemic response that was characterized by a bilateral decrease in synergies activation in the first epoch of both AD and PA, as reflected by the absence, in both AD and PA of synergy amplitude up-modulation. In fact, in both the Angle and Length experiments, we observed, in the first epoch of BL, an increase in RMS in all the synergies (**Figure 9A, 9B** and **10**) that reflects the task requirements to reach the desired speed and power output as soon as possible. As this requirement is left unchanged during the AD and PA phases

of experiments, the same behavior would have been expected also in the first epoch of such phases, as observed in the Angle experiment. Instead, we observe APs that are remarkably close to the average BL ones during the first epochs of both AD and PA (**Figure 10**). The behavior we observe in the Length experiment is more consistent with the modulation of a feedback response rather than a motor adaptation. Locomotor adaptations have been shown to be constituted by both feedback and feedforward components (Lam et al. 2006; Reisman et al. 2005). The former are fast adjustments that do not yield an aftereffect once the perturbation is removed, while the latter are slower adjustments that are progressively learned, consistently with the update of a motor plan, and produce an after effect in the opposite direction. In this interpretation in the Length experiment we observe, during both AD and PA, an initial reflex response that is quickly discarded in the first few cycles of both phases. Nevertheless, the fact that this response is observed in all synergies (thus seemingly in all muscles) on both sides poses some doubts on this hypothesis, since spinal reflex are usually very specific (Pearson 2004; Schillings et al. 2000; van der Linden et al. 2007). An alternative explanation could be that only a subset of muscles is affected by the reflex activity, while the others simply respond to an alteration in task demands that is caused by both the reflex and the asymmetry. However, the data we present cannot confirm either of these hypothesis and a clear interpretation of the results we observe in the Length experiment remains elusive.

Synergy modules are robust to the asymmetries. Regardless of the neural strategy employed to counteract the asymmetry, the neuromuscular changes in our experiments are exclusively observed in the activation patterns of the synergies while the shapes of the modules remain consistent through the different phases of the experiments. Although our statistical analysis on the modification of the motor modules cannot be conclusive due to the small effect size (e.g. changes are only observed in brief parts of each cycle while modules capture the whole cycle, similarly to what argued in (Maclellan et al. 2014)), our results are in accordance with the majority of previous literature that has shown that synergistic modules, as expressed by the W parameter in the NNMF algorithm, are robust across different tasks and task demands. During lower limb movements, synergy modules have been shown to be robust through different walking conditions (Chia Bejarano et al. 2017; Courtine et al. 2006; Oliveira

et al. 2016), balance perturbations (Oliveira et al. 2013; Torres-Oviedo et al. 2006), cycling conditions (De Marchis et al. 2013; Hug et al. 2011), fatigue (Castronovo et al. 2018; Turpin et al. 2011) and to be shared across different tasks (Barroso et al. 2014; Chvatal and Ting 2013). Similar results have also been observed during motor adaptations. Studies on visuomotor rotations in the upper limbs have demonstrated that APs are rotated while modules remain consistent when adapting to different visual perturbations (Berger et al. 2013; De Marchis et al. 2018; Gentner et al. 2013) and similar results have been also observed during split-belt treadmill experiments (Maclellan et al. 2014). Our results seem to suggest a rotation effect in the APs of the muscle synergies during the Angle experiment similar to the one observed during visuomotor rotations (De Marchis et al. 2018; Gentner et al. 2013). Nevertheless, while for the temporal asymmetry it was expected that a potential adaptation would have been explained only through a modification of the APs, in the Length experiment it could have been expected that the asymmetry would have altered the relative contribution of the different muscles to the task. In fact, Ranganathan et al. (Ranganathan et al. 2016) showed that adjustments to different kinematical demands can be obtained by changing the modular structure of the synergies in a conceptually similar task performed while walking in the Lokomat device. Instead, we observed an amplitude modulation of the same muscle synergies, possibly due to the fact that the asymmetry we introduce is very small with respect to the altered task demands that subjects experienced in the work by Ranganathan and colleagues. This comparison would suggest that APs are preferentially modulated also in the presence of small changes in the muscular dynamics of the task demands.

Conclusions. The results herein presented show that motor adaptations in the lower limbs are present in response to small temporal asymmetries during cycling, but not in response to spatial asymmetries. The adaptions we observe are present when balance is not directly compromised and when the kinematic error cannot be compensated for. Our results suggest that the neural circuits controlling the timing of the legs during repetitive movements are hardwired to maintain specific symmetry features in the unilateral muscular activation patterns.

Acknowledgements

We thank Magdalena Gontarz for her contribution to the data collection. \

Grants

This work was partially funded by the UCD seed grants SF1303 and SF1622

References

Abe D, Muraki S, Yanagawa K, Fukuoka Y, and Niihata S. Changes in EMG characteristics and metabolic energy cost during 90-min prolonged running. *Gait Posture* 26: 607-610, 2007.

Barroso FO, Torricelli D, Moreno JC, Taylor J, Gomez-Soriano J, Bravo-Esteban E, Piazza S, Santos C, and Pons JL. Shared muscle synergies in human walking and cycling. *J Neurophysiol* 112: 1984-1998, 2014.

Berger DJ, Gentner R, Edmunds T, Pai DK, and d'Avella A. Differences in adaptation rates after virtual surgeries provide direct evidence for modularity. *J Neurosci* 33: 12384-12394, 2013.

Caggiano V, Leiras R, Goni-Erro H, Masini D, Bellardita C, Bouvier J, Caldeira V, Fisone G, and Kiehn O. Midbrain circuits that set locomotor speed and gait selection. *Nature* 553: 455-460, 2018.

Cajigas I, Koenig A, Severini G, Smith M, and Bonato P. Robot-induced perturbations of human walking reveal a selective generation of motor adaptation. *Science Robotics* 2: eaam7749, 2017.

Castronovo AM, De Marchis C, Schmid M, Conforto S, and Severini G. Effect of Task Failure on Intermuscular Coherence Measures in Synergistic Muscles. *Applied Bionics and Biomechanics* 2018: 2018.

Chia Bejarano N, Pedrocchi A, Nardone A, Schieppati M, Baccinelli W, Monticone M, Ferrigno G, and Ferrante S. Tuning of Muscle Synergies During Walking Along Rectilinear and Curvilinear Trajectories in Humans. *Ann Biomed Eng* 45: 1204-1218, 2017.

Choi JT, and Bastian AJ. Adaptation reveals independent control networks for human walking. *Nat Neurosci* 10: 1055-1062, 2007.

Chvatal SA, and Ting LH. Common muscle synergies for balance and walking. *Front Comput Neurosci* 7: 48, 2013.

Courtine G, Papaxanthis C, and Schieppati M. Coordinated modulation of locomotor muscle synergies constructs straight-ahead and curvilinear walking in humans. *Exp Brain Res* 170: 320-335, 2006.

d'Avella A, Saltiel P, and Bizzi E. Combinations of muscle synergies in the construction of a natural motor behavior. *Nat Neurosci* 6: 300-308, 2003.

De Marchis C, Di Somma J, Zych M, Conforto S, and Severini G. Consistent visuomotor adaptations and generalizations can be achieved through different rotations of robust motor modules. *Scientific Reports* in press: 2018.

De Marchis C, Schmid M, Bibbo D, Castronovo AM, D'Alessio T, and Conforto S. Feedback of mechanical effectiveness induces adaptations in motor modules during cycling. *Front Comput Neurosci* 7: 35, 2013.

De Marchis C, Severini G, Castronovo AM, Schmid M, and Conforto S. Intermuscular coherence contributions in synergistic muscles during pedaling. *Exp Brain Res* 233: 1907-1919, 2015.

Dominici N, Ivanenko YP, Cappellini G, d'Avella A, Mondi V, Cicchese M, Fabiano A, Silei T, Di Paolo A, Giannini C, Poppele RE, and Lacquaniti F. Locomotor primitives in newborn babies and their development. *Science* 334: 997-999, 2011.

Drew T. Motor cortical cell discharge during voluntary gait modification. *Brain Res* 457: 181-187, 1988.

Emken JL, Benitez R, Sideris A, Bobrow JE, and Reinkensmeyer DJ. Motor adaptation as a greedy optimization of error and effort. *J Neurophysiol* 97: 3997-4006, 2007.

Emken JL, and Reinkensmeyer DJ. Robot-enhanced motor learning: accelerating internal model formation during locomotion by transient dynamic amplification. *IEEE Trans Neural Syst Rehabil Eng* 13: 33-39, 2005.

Finley JM, Bastian AJ, and Gottschall JS. Learning to be economical: the energy cost of walking tracks motor adaptation. *J Physiol* 591: 1081-1095, 2013.

Frigon A, Hurteau MF, Thibaudier Y, Leblond H, Telonio A, and D'Angelo G. Split-belt walking alters the relationship between locomotor phases and cycle duration across speeds in intact and chronic spinalized adult cats. *J Neurosci* 33: 8559-8566, 2013.

Gentner R, Edmunds T, Pai DK, and d'Avella A. Robustness of muscle synergies during visuomotor adaptation. *Front Comput Neurosci* 7: 120, 2013.

Grillner S. The motor infrastructure: from ion channels to neuronal networks. *Nat Rev Neurosci* 4: 573-586, 2003.

Hamley EJ, and Thomas V. Physiological and postural factors in the calibration of the bicycle ergometer. *J Physiol* 191: 55P-56P, 1967.

Hermens HJ, Freriks B, Merletti R, Stegeman D, Blok J, Rau G, Disselhorst-Klug C, and Hägg G. European recommendations for surface electromyography. *Roessingh research and development* 8: 13-54, 1999.

Hug F, Turpin NA, Couturier A, and Dorel S. Consistency of muscle synergies during pedaling across different mechanical constraints. *J Neurophysiol* 106: 91-103, 2011.

Ivanenko YP, Cappellini G, Dominici N, Poppele RE, and Lacquaniti F. Coordination of locomotion with voluntary movements in humans. *J Neurosci* 25: 7238-7253, 2005.

Ivanenko YP, Poppele RE, and Lacquaniti F. Five basic muscle activation patterns account for muscle activity during human locomotion. *J Physiol* 556: 267-282, 2004.

Jensen L, Prokop T, and Dietz V. Adaptational effects during human split-belt walking: influence of afferent input. *Exp Brain Res* 118: 126-130, 1998.

Jordan LM, Liu J, Hedlund PB, Akay T, and Pearson KG. Descending command systems for the initiation of locomotion in mammals. *Brain Res Rev* 57: 183-191, 2008.

Kandel ER, Schwartz JH, Jessell TM, Siegelbaum SA, and Hudspeth AJ. *Principles of neural science*. McGraw-hill New York, 2000.

Kawato M. Internal models for motor control and trajectory planning. *Curr Opin Neurobiol* 9: 718-727, 1999.

Kiehn O. Decoding the organization of spinal circuits that control locomotion. *Nat Rev Neurosci* 17: 224-238, 2016.

Kiehn O. Locomotor circuits in the mammalian spinal cord. *Annu Rev Neurosci* 29: 279-306, 2006.

Lacquaniti F, Ivanenko YP, and Zago M. Patterned control of human locomotion. *J Physiol* 590: 2189-2199, 2012.

Lam T, Anderschitz M, and Dietz V. Contribution of feedback and feedforward strategies to locomotor adaptations. *J Neurophysiol* 95: 766-773, 2006.

Lee DD, and Seung HS. Algorithms for non-negative matrix factorization. In: *Advances in neural information processing systems*2001, p. 556-562.

Maclellan MJ, Ivanenko YP, Massaad F, Bruijn SM, Duysens J, and Lacquaniti F. Muscle activation patterns are bilaterally linked during split-belt treadmill walking in humans. *J Neurophysiol* 111: 1541-1552, 2014.

Malone LA, Bastian AJ, and Torres-Oviedo G. How does the motor system correct for errors in time and space during locomotor adaptation? *J Neurophysiol* 108: 672-683, 2012.

McCrea DA, and Rybak IA. Organization of mammalian locomotor rhythm and pattern generation. *Brain Res Rev* 57: 134-146, 2008.

McDonagh MJ, and Duncan A. Interaction of pre-programmed control and natural stretch reflexes in human landing movements. *J Physiol* 544: 985-994, 2002.

Oliveira AS, Gizzi L, Ketabi S, Farina D, and Kersting UG. Modular Control of Treadmill vs Overground Running. *PLoS One* 11: e0153307, 2016.

Oliveira AS, Silva PB, Lund ME, Gizzi L, Farina D, and Kersting UG. Effects of perturbations to balance on neuromechanics of fast changes in direction during locomotion. *PLoS One* 8: e59029, 2013.

Pearson KG. Generating the walking gait: role of sensory feedback. *Prog Brain Res* 143: 123-129, 2004.

Peveler WW, Pounders JD, and Bishop PA. Effects of saddle height on anaerobic power production in cycling. *J Strength Cond Res* 21: 1023-1027, 2007.

Prokop T, Berger W, Zijlstra W, and Dietz V. Adaptational and learning processes during human split-belt locomotion: interaction between central mechanisms and afferent input. *Exp Brain Res* 106: 449-456, 1995.

Ranganathan R, Krishnan C, Dhaher YY, and Rymer WZ. Learning new gait patterns: Exploratory muscle activity during motor learning is not predicted by motor modules. *Journal of biomechanics* 49: 718-725, 2016.

Reisman DS, Block HJ, and Bastian AJ. Interlimb coordination during locomotion: what can be adapted and stored? *J Neurophysiol* 94: 2403-2415, 2005.

Scheidt RA, Dingwell JB, and Mussa-Ivaldi FA. Learning to move amid uncertainty. *Journal of Neurophysiology* 86: 971-985, 2001.

Schillings AM, van Wezel BM, Mulder T, and Duysens J. Muscular responses and movement strategies during stumbling over obstacles. *J Neurophysiol* 83: 2093-2102, 2000.

Shadmehr R, and Mussa-Ivaldi FA. Adaptive representation of dynamics during learning of a motor task. *J Neurosci* 14: 3208-3224, 1994.

Takakusaki K. Neurophysiology of gait: from the spinal cord to the frontal lobe. *Mov Disord* 28: 1483-1491, 2013.

Torres-Oviedo G, Macpherson JM, and Ting LH. Muscle synergy organization is robust across a variety of postural perturbations. *J Neurophysiol* 96: 1530-1546, 2006.

Torres-Oviedo G, Vasudevan E, Malone L, and Bastian AJ. Locomotor adaptation. *Prog Brain Res* 191: 65-74, 2011.

Tresch MC, Saltiel P, and Bizzi E. The construction of movement by the spinal cord. *Nat Neurosci* 2: 162-167, 1999.

Turpin NA, Guevel A, Durand S, and Hug F. Fatigue-related adaptations in muscle coordination during a cyclic exercise in humans. *J Exp Biol* 214: 3305-3314, 2011.

van der Linden MH, Marigold DS, Gabreels FJ, and Duysens J. Muscle reflexes and synergies triggered by an unexpected support surface height during walking. *J Neurophysiol* 97: 3639-3650, 2007.

Zhong G, Shevtsova NA, Rybak IA, and Harris-Warrick RM. Neuronal activity in the isolated mouse spinal cord during spontaneous deletions in fictive locomotion: insights into locomotor central pattern generator organization. *J Physiol* 590: 4735-4759, 2012.